Mem. Natl Inst. Polar Res., Spec. Issue, **47**, 26–35, 1987

NONLINEAR EFFECT FOR THE OMEGA SIGNALS IN THE AURORAL IONOSPHERE BY ROCKET OBSERVATIONS

Masanori NISHINO[1] and Eigil UNGSTRUP[2]

[1]*Research Institute of Atmospherics, Nagoya University, 13, Honohara 3-chome, Toyokawa 442*
[2]*Danish Space Research Institute, Lundtoftevej 7, DK-2800 Lyngby, Denmark*

Abstract: Electromagnetic waves at 10.2 and 13.6 kHz from the Omega transmitter located in the northern Norway were observed on board four rocket payloads. Among these Omega signals, an unusual feature has been found for three payloads; the signals which ordinarily show double spin modulation of twice the rocket spin frequency were converted to single spin modulation in the altitude range of 70–115 km of the ionosphere, and the conversion took place for deep spin modulated signals with a weak intensity. It is concluded that the conversion was caused by a nonlinear effect of the Langmuir characteristic in the ionospheric plasma which indicated approximately a square root function.

1. Introduction

According to the rocket program of the Danish Space Research Institute, a series of rockets were launched in northern Scandinavia in order to study VLF emissions associated with aurora. The observational results have been reported in papers by IVERSEN *et al.* (1968) and UNGSTRUP (1971, 1975, 1980). In these four rocket observations, we could observe the signals from the Omega transmitter station, emitting the two different frequencies of 10.2 and 13.6 kHz, and further noticed an unusual feature for the three observations: the Omega signals which ordinarily show double spin modulation of twice the rocket spin frequency were converted to single spin modulation in the altitude range of 70–115 km of the ionosphere.

CARTWRIGHT (1964) measured the Doppler shift of the 10.2 kHz Omega signal in the nighttime ionosphere by a rocket observation. UNGSTRUP *et al.* (1978) and NEUBERT *et al.* (1983) observed the Omega signals by the GEOS-1 satellite in order to study the propagation aspects in the magnetospheric plasma. BELL *et al.* (1981) observed the triggered VLF emissions associated with the nonducted Omega signals by the ISEE-1 satellite, and also INAN and BELL (1985) observed the spectral broadening of the Omega signals by the DE-1 satellite. As described above, the observations of the Omega signals by the space vehicles provide valuable information to understand the dynamics of the ionospheric and magnetospheric plasma. However, as far as we know, we have never found papers describing the unusual feature of single spin modulation.

The purpose of this paper is to present the unusual feature of the Omega signals observed by the rockets, and to propose a conversion mechanism from the double to the

Table 1. Data of the launching for the four rockets.

	F13	C31/1	C31/2	S70/2
Launching place	Andöya rocket range	Esrange, Sweden	Esrange, Sweden	Esrange, Sweden
Geographic coordinate	69.30°N, 16.03°E	67.90°N, 21.11°E	67.90°N, 21.11°E	67.90°N, 21.11°E
L-value	6.32	5.51	5.51	5.51
Invariant latitude	66.56°	64.79°	64.79°	64.79°
Launching date	26 June 1966	26 November 1967	6 December 1967	25 November 1971
Launching time	2147: 13 UT	1947: 22 UT	2121: 12 UT	1713: 05 UT
Approximate flight time	6 min	6 min	6 min	7 min
Maximum altitude	138.1 km	125.6 km	128.5 km	175.0 km
Launching direction	320°	358°	354°	343°

single spin modulations.

Table 1 shows the data of the launching places, launching times etc. for the four rockets concerned.

2. Instrumentation

The antennas used for the observations of the Omega signals were 1.0 m^2 loops with their normal perpendicular to rocket spin axis for the three payloads (C31/1, C31/2 and S70/2), and a 0.42 m^2 loop for the F13 payload. The four loop antennas consisted of 20 turns of stranded copper wire, and they were electrostatically shielded. For the S70/2 payload, the loop antenna was connected to a preamplifier input through a transformer with a 1: 30 turn ratio. On the other hand, the loop antennas for the other payloads (F13, C31/1 and C31/2) were directly connected to the respective preamplifier, as is shown in the diagram of Fig. 1. Wide band receivers on board the four rockets have the observing frequency band of 0.5–10 kHz, and for only the F13 payload a narrow band receiver tuned at 13.6 kHz ($\Delta f = 100$ Hz) was also equipped. The antennas of the three payloads (F13, C31/1 and C31/2) were deployed at 57 s after launch when the payloads were 57 km altitude, and the antenna of the S70/2 payload was deployed at 69 s after launch at 69 km altitude.

For data analysis we obtained spin modulated amplitude at 10.2 kHz through a

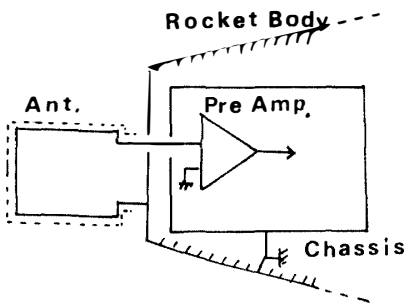

Fig. 1. Circuit diagram of the antenna to preamplifier input for the three payloads (F13, C31/1 and C31/2).

narrow band amplifier ($\Delta f = 100$ Hz) and a detector with fast charging time (<0.1 s) from the wide band tape data (0.5–10 kHz) (see Figs. 2 and 3).

3. Observations

The Omega transmitter from which the signals have been observed on the four rockets is located in the northern part of Norway at 66°25′15″N, 13°09′10″E which is 343 km distance and 202° azimuthal direction from the launching place at Andöya, and also 390 km distance and 249° azimuthal direction from the launching place at Esrange. The transmitter emitted VLF waves on the two different frequencies: 10.2 kHz with 0.9 s duration and 13.6 kHz with 1.1 s duration once during the repetition period of 10 s with a radiation efficiency of about 5% of the transmitter power of 10 kW.

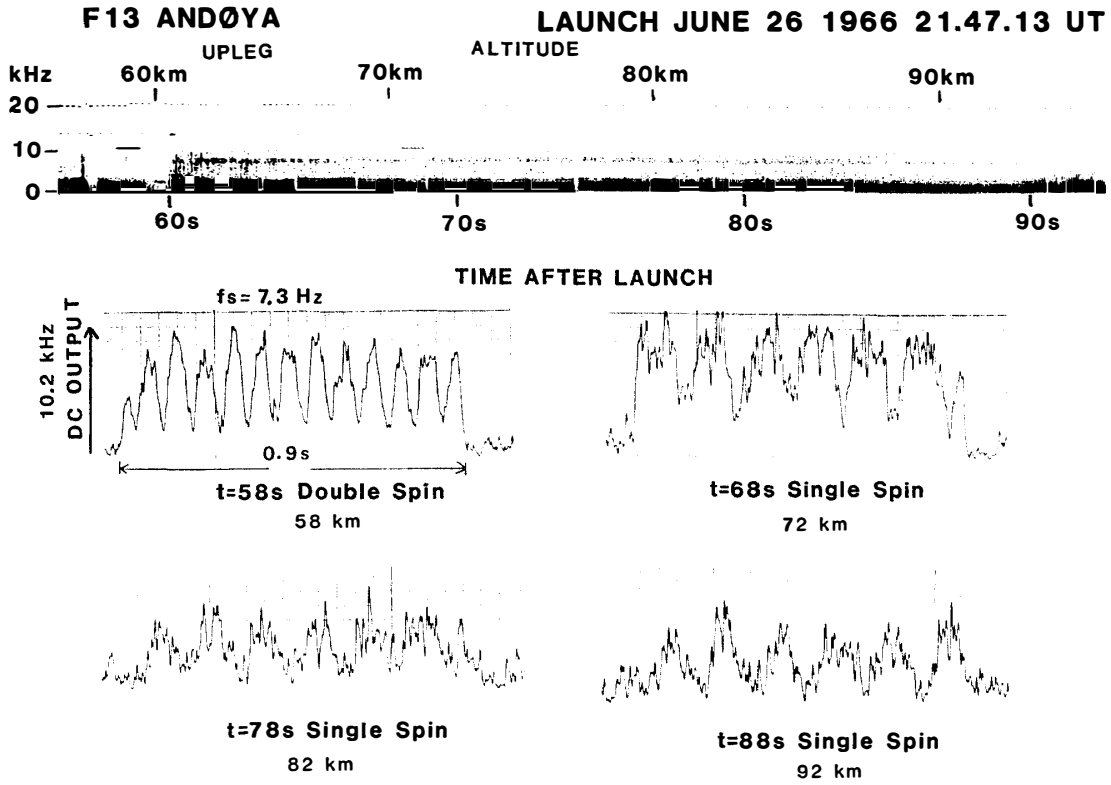

Fig. 2. The Omega signals in the wide band spectrum (≤ 20 kHz) and the corresponding spin modulation waveforms at 10.2 kHz on the upleg for the F13 payload. The spin frequency of the payload is near 7.3 Hz.

Figure 2 shows a wide band spectrum developed by a spectral analyzer (<20 kHz) in which the Omega signals were observed and the corresponding spin modulated amplitude at 10.2 kHz for the F13 payload. The amplitude is shown by an arbitrary voltage scale. The spin modulated amplitude shows the ordinary double spin of twice the rocket spin frequency ($f_s \sim 7.3$ Hz) at 58 s (58 km altitude) just after the antenna deployment. However, it evidently shows single spin characteristic at 68 s (72 km altitude), as also seen in the spectrum. The single spin modulations appeared until

98 s (100 km altitude) on the upleg, although the amplitude waveforms are not presented after 98 s. Above 100 km altitude the modulations are ambiguous whether they are double or single spin, due to the contamination by background VLF emissions, and they show no spin around the apex of the trajectory. From the apex to 115 km altitude on the downleg, they showed no spin or ambiguous spin, and thereafter the single spin appeared again in the altitude range from 115 to 90 km. The observed intensities in the ionosphere above 90 km altitude are estimated to be weak ones of the order of 10–30 μV/m, referring to narrow band intensity at 13.6 kHz calibrated on the ground.

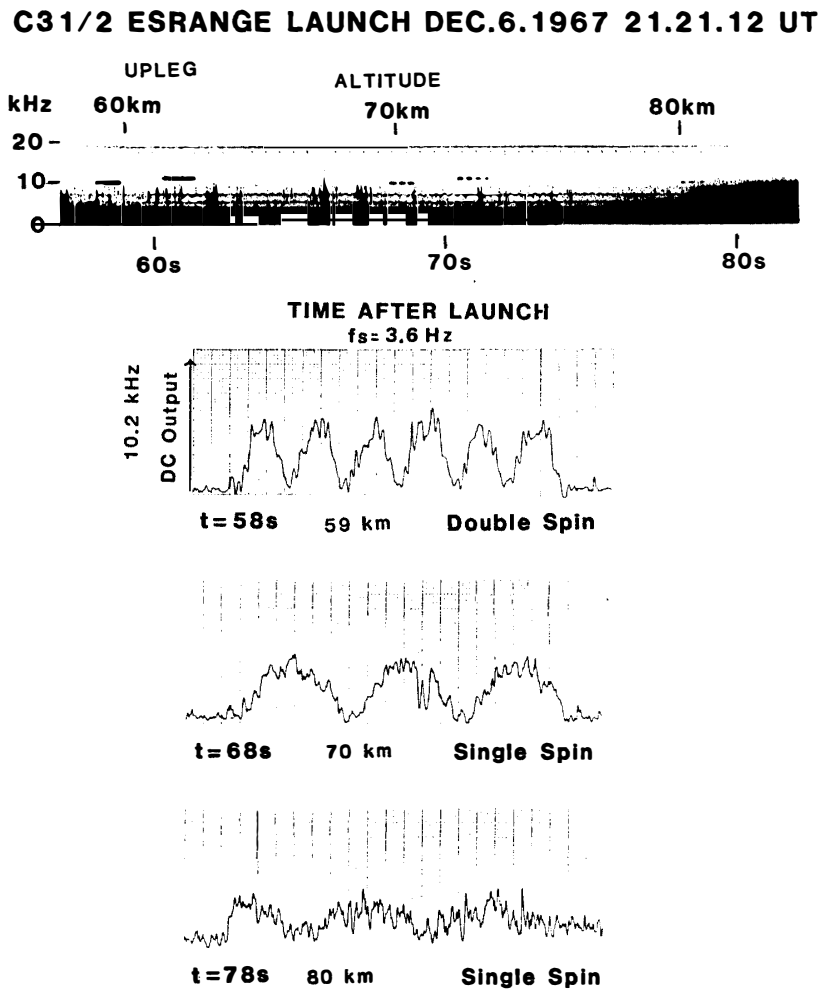

Fig. 3. The Omega signals in the wide band spectrum ($\leq$20 kHz) and the corresponding spin modulation waveforms at 10.2 kHz on the upleg for the C31/2 payload. The spin frequency of the payload is near 3.6 Hz.

Figure 3 shows a wide band spectrum and the corresponding spin modulated amplitude for the C31/2 payload. The modulation shows the double spin ($f_s \sim 3.6$ Hz) at 58 s (59 km altitude), but it evidently shows the single spin at 68 s (70 km altitude) and also at 78 s (80 km altitude) on the upleg. The single spin modulation at 13.6

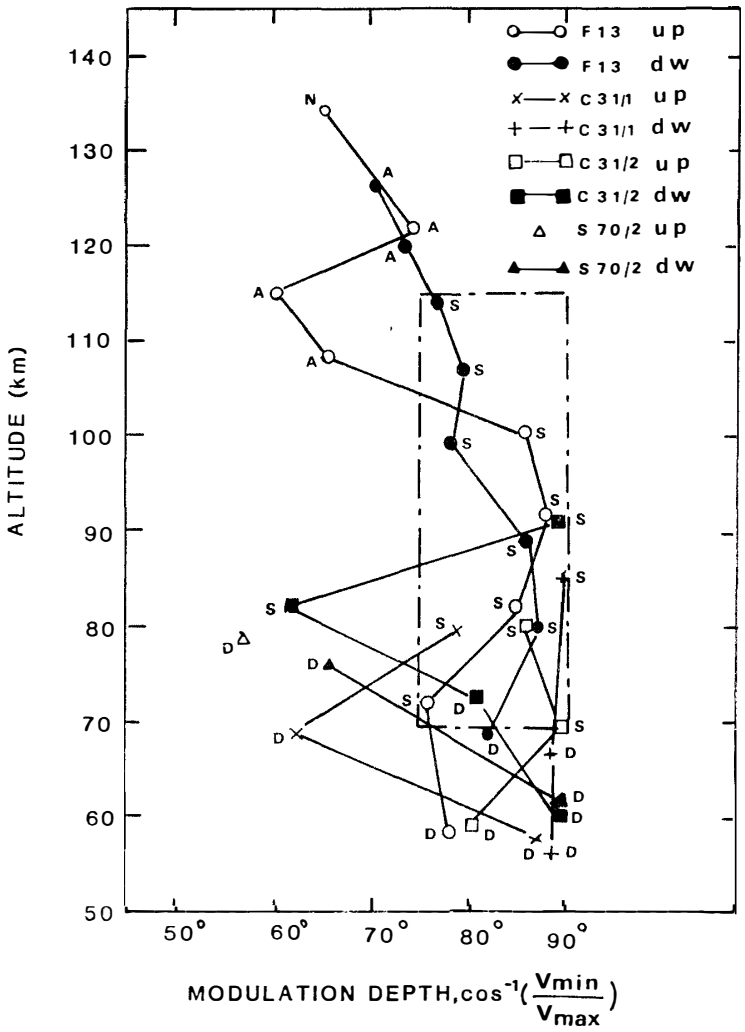

Fig. 4. Profiles of the modulation depths of the spin modulation waveforms at 10.2 kHz for the four payloads with altitude. The modulation depths are represented by arccosine of the ratio of minimum to maximum of the modulation amplitude. Symbols shown is D for double spin modulation, S for single spin modulation, A for the ambiguous modulation and N for no spin.

kHz is also found at 70 s (72 km altitude) in the spectrum. No Omega signal was observed above 80 km altitude on the upleg and above 90 km on the downleg, due to the contamination by strong VLF emissions.

Figure 4 shows the profile of the modulation depth for the spin modulated signals observed by the four payloads with altitudes, where the depth is represented by arccosine of the ratio of minimum to maximum of the modulated amplitude. Notation of the spin modulation is depicted by four symbols (D: double, S: single, A: ambiguous and N: no spin). It is found from this figure that the modulated signals of the three payloads (F13, C31/1 and C31/2) which showed the ordinary double spin modulation in the subionospheric region below 70 km altitude were converted to the single spin in the ionospheric region of 70–115 km altitude. Besides, it should be noted that the conversion took place for deep spin modulated signals except one for the C31/2 down-

leg, as is shown by a frame in the figure. The modulation (only F13) shows the ambiguous spin or no spin above 115 km altitude. On the other hand, the modulation for the S70/2 payload always show double spin during the flight.

4. Discussion

First we discuss the conversion mechanism from the double spin to the single spin modulations. A loop antenna, in an ideal condition, picks up a balanced component of the induced signal. However, on the loop antennas on board the three rockets (F13, C31/1 and C31/2), one terminal of the loop element was connected to the input of the preamplifier in an electronics chassis, while another one was connected to the rocket body, as is shown in Fig. 1. It is naturally guessed from this figure that imperfection for the balance of the antenna structure and unreasonable connection between the antenna and the preamplifier cause the unbalanced (vertical) effect of the antenna. As the result, the antenna might pick up composite of the balanced and the unbalanced components. In this case, the signal strength of the balanced component is relatively weak because of the small effective length (~ 2 mm), then the unbalanced component induced by the vertical effect seem to be rather dominant. Therefore it is suggested that the vertical effect which is equivalent to the electric field antenna worked as the Langmuir probe in the ionospheric plasma.

As was seen from the amplitude envelope of the received Omega signal in Figs. 2 and 3, the signals show the double spin modulation below 70 km altitude in the sub-ionospheric region. Then the envelope of the signal induced by the electric antenna is expressed as follows;

$$\langle V^2(t)\rangle = K_1\{1+M\cos(2\omega_s t)\}\,, \tag{1}$$

where ω_s is the spin frequency. The parameters K_1 and M are functions of the wave normal direction, the wave polarization and the antenna orientation in the ionospheric plasma (SONWALKAR and INAN, 1986).

It is well known that the current-voltage ($J-V$) characteristic measured by the Langmuir probe is given as follows;

$$J = S_A J_{se} \exp\{e(V-V_S)/\kappa T_e\} - S_A J_{si}\,, \tag{2}$$

where S_A, J_{se}, J_{si}, V_s, κ, T_e and e are the surface area of the probe, electron saturation current density, ion saturation current density, space potential, Boltzmann's constant, electron temperature and electronic charge, respectively, and the ($J-V$) characteristic is drawn by a solid curve in Fig. 5. It should be noticed that the nonlinear Langmuir curve is apparently similar to the one of the square root function, particularly on the curvature in the limited voltage range between V_s and V_f (floating potential). So, we adopt the following equation as the approximate one of the Langmuir nonlinear characteristic.

$$J \propto K_2(V-V_S)^{1/2}\,. \tag{3}$$

We operate the eq. (1) to the variance $(V-V_s)^{1/2}$ in the eq. (3), then the amplitude of the Langmuir current is

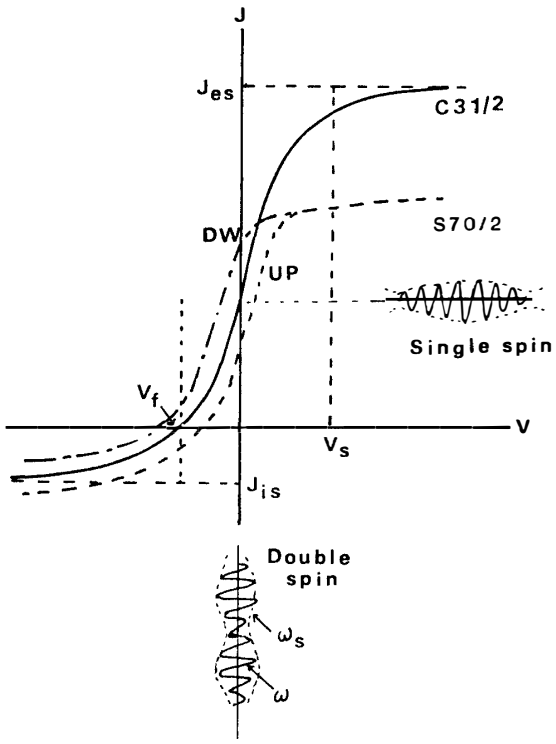

Fig. 5. Voltage-current characteristic of the Langmuir probe to explain the conversion mechanism to single spin modulation and to interprete no single spin modulation for the S70/2 payload.

$$J_{\mathrm{amp}} \propto K_1 K_2 \{1+M \cos(2\omega_s t)\}^{1/2} . \tag{4}$$

This equation is converted to the following eq. (5) by the use of a familiar trigonometric formula,

$$J_{\mathrm{amp}} \propto K_1 K_2 \{(1-M)+2M \cos^2(\omega_s t)\}^{1/2} . \tag{5}$$

If M is nearly equal 1 which means deep spin modulated signals, the amplitude of the current is converted to the single spin modulation (ω_s), as follows;

$$J_{\mathrm{amp}} \propto \sqrt{2}\, K_1 K_2 \{\cos(\omega_s t)\} . \tag{6}$$

From the above description and the illustration of Fig. 5, we can understand that the conversion takes place only for the deep spin modulated signals, which is consistent with the observation result of the single spin modulation in the lower ionosphere, as is shown in Fig. 4.

For the wave penetration into the lower ionosphere from the ground transmitter, the wave polarization is calculated by the full wave method (PITTEWAY and JESPERSEN,

Table 2. Polarization parameters of the penetrated waves in the lower ionosphere.

Altitude	Incident angle	Azimuthal angle	$\tan^{-1}\lvert a\rvert$	$\arg(a)$
70 km	77°	205°	49.7°	13.3°
80 km	30°	205°	64.8°	74.0°
90 km	20°	205°	67.5°	83.6°

1966). Table 2 shows a calculated result for the F13 payload by using *in situ* measurement of the electron density. The incident angle into the ionosphere at 70 km altitude is determined by the distance (343 km) from the transmitter, and the incident angles at 80 and 90 km altitudes are roughly estimated from the refractive index surface calculated from the Appleton-Hartree equation neglecting the collision effect. The azimuthal angles indicate the clockwise ones from the geomagnetic north. $\tan^{-1}|a|$ and arg (a) indicate the polarization parameters in the plane perpendicular to the wave vector. It is found from this result that the Omega waves show definitely elliptic polarization at 70 and 80 km altitudes in the lower ionosphere, but the waves become nearly circular polarization above 90 km altitude. The small incident angle and the circular polarization cause the difficulty of conversion because of shallow spin modulation of the received signal, whereas the single spin modulations were observed until 115 km altitude for the F13 payload. This inconsistency will be discussed further taking account of the relationship between the wave arrival condition and the antenna orientation.

A different nonlinear effect was observed in the ionospheric plasma only for the F13 payload: The amplitude modulated RF waves ($\sim$MHz) from the nearby broadcasting station were demodulated around the altitude of 130 km both on the upleg and downleg. The physical mechanism of this nonlinear effect has already been clarified with the use of a laboratory simulation experiment by KAWASHIMA (1968). As the result, the antenna worked as the ordinary resonance probe in the ionospheric plasma. The large RF waves resonating in the inductive plasma and capacitive sheath surrounding the probe were rectified by the nonlinear current-voltage characteristic of the sheath.

BUTLER and KINO (1963) carried out a laboratory experiment by which the large amplitude ($\sim$200 V) of VLF signal ($\sim$50 kHz) were clipped due to the ion sheath formed near the inner walls in the plasma discharge tube. These experiments indicated that large amplitude signals caused nonlinear effect due to the plasma and the ion sheath. However, it must be noted that the conversion from double spin to single modulation of the weak Omega signals indicates the nonlinear effect of the plasma itself through the Langmuir characteristic.

Next we discuss a problem why no single spin modulation was observed for the S70/2 payload. As described in the instrument, the loop antenna of the S70/2 payload was connected to the transformer, then it might pick up completely the balanced component of the induced signal. However, it may be considered that different conditions caused no conversion. Below we discuss it by comparing the launching conditions between the S70/2 and the C31/2 payloads.

Both rockets were launched in the winter nighttime from Esrange, as is shown in Table 1. The precession angles to the rocket axis in the altitude range of 70–92 km, where the single spin modulations were observed for C31/2, were 147–162° for C31/2 and 153–164° for S70/2, respectively. It is estimated that the wave incidence on the antenna is similar for the both payloads.

Contrary to the conversion described above, no conversion suggests that the nonlinear Langmuir characteristic is not approximately given by the square root function in the limited voltage range between V_s and V_f. The electron temperature which

determines the gradient of the Langmuir characteristic shows no significant change in the lower ionosphere below about 95 km on the quiet day (corresponding to S70/2) and the disturbed day (corresponding to C31/2) (SCHLEGEL *et al.*, 1980). Therefore, we can imagine that no conversion is related to the difference between the two rocket velocities. The vertical rocket velocities were 1.0 km/s for C31/2 and 1.4 km/s for S70/2 at 75 km altitude on the upleg, and were 1.0 km/s for C31/2 and 0.6 km/s for S70/2 at 80 km altitude on the downleg.

The floating potential V_f on the Langmuir characteristic shown in Fig. 5, in principle, equals $\kappa T_e/e \ln (v_i/v_e)$, where v_e and v_i are electron thermal velocity and ion thermal velocity, respectively, if the probe size is negligibly small for the rocket. Actually, this potential changes by the anisotropic character of the ion velocities due to the rocket supersonic velocity which acts to increase the ion current by a factor proportional to the ionic Mach number (v_s/v_i), defined by the ratio of the rocket velocity to the ion thermal velocity. Ion thermal velocity is typically given by $v_i=0.3$ km/s at 75 km altitude (GIRAUD and PETIT, 1978), which is smaller than the rocket velocities. And also, the electron thermal velocity is typically given by $v_e=100$ km/s at 75 km altitude. Then, the floating potential for S70/2 is estimated to be shifted by 7.3% in the positive direction on the upleg and by 11.8% in the negative direction on the downleg, referring to the floating potential for C31/2. Besides, since the measured electron density for S70/2 is lower by about a factor of 20, comparing with that for C31/2 at 75 km altitude, electron saturation current on $(J-V)$ characteristic for S70/2 becomes smaller than that for C31/2. Therefore, it seems that the above these effects caused the change of the nonlinear characteristic which results in no conversion for S70/2, as is schematically shown in Fig. 5.

5. Conclusion

We have presented the unusual feature of the single spin modulation for the Omega signals observed by the three payloads (F13, C31/1 and C31/2) in the ionosphere. This phenomena were observed in the altitude range of 70–115 km for the deep spin modulated signals. It is concluded that the conversion was caused by the nonlinear characteristic of the Langmuir probe in the ionospheric plasma which indicated approximately the square root function.

We have discussed the cause of no conversion for the S70/2 payload. The cause may be attributed to the change of the nonlinear characteristic due to the relative increase (decrease) of the rocket velocity and the relative decrease of background electron density in the lower ionosphere.

Acknowledgments

The authors wish to express their gratitude to Prof. A. IWAI and Dr. Y. TANAKA for their continuous encouragement. Thanks are also due to Drs. F. PRIMDAHL and I. B. IVERSEN of Danish Space Research Institute for their valuable comments.

One of authors (M. N.) has beeen supported by a Grant-in-Aid for overseas scientific research from the Ministry of Education, Science and Culture of Japan.

References

BELL, T. F., INAN, U. S. and HELLIWELL, R. A. (1981): Non ducted coherent VLF waves and associated emissions observed on the ISEE-1 satellite. J. Geophys. Res., **86**, 4649–4670.

BUTLER, H. S. and KINO, G. S. (1963): Plasma sheath formation by radio-frequency fields. Phys. Fluids, **6**, 1346–1355.

CARTWRIGHT, D. G. (1964): A 10-kilocycle per second doppler observation of the intermediate layer of the night time ionosphere. J. Geophys. Res., **69**, 4031–4035.

GIRAUD, A. and PETIT, M. (1978): Ionospheric Techniques and Phenomena. Dordrecht, D. Reidel, 264 p. (Geophysics and Astrophysics Monographs, Vol. 13).

INAN, U. S. and BELL, T. E. (1985): Spectral broadening of VLF transmitter signals observed on DE-1; A quasi-electrostatic phenomena? J. Geophys. Res., **90**, 1771–1775.

IVERSEN, I. B., OLSEN, O. H. and UNGSTRUP, E. (1968): Observation of VLF-radio noise in the ionosphere during an auroral absorption event. Ann. Geophys., **24**, 313–316.

KAWASHIMA, N. (1968): Demodulation of amplitude modulated RF waves in a plasma at resonance. Radio Sci., **3**, 377–381.

NEUBERT, T., UNGSTRUP, E. and BAHNSEN, A. (1983): Observation on the GEOS-1 satellite of whistler mode signals transmitted by the Omega navigation system transmitter in Northern Norway. J. Geophys. Res., **88**, 4015–4025.

PITTEWAY, M. L. V. and JESPERSEN, J. L. (1966): A numerical study of the excitation, internal reflection and limiting polarization of whistler waves in the lower ionosphere. J. Atmos. Terr. Phys., **28**, 17–43.

SCHLEGEL, K., KOHL, H. and RINNERT, K. (1980): Temperatures and collision frequency in the polar *E* region measured with the incoherent scatter technique. J. Geophys. Res., **85**, 710–714.

SONWALKER, V. S. and INAN, U. S. (1986): Measurements of Siple transmitter signals on the DE 1 satellite; Wave normal direction and antenna effective length. J. Geophys. Res., **91**, 154–164.

UNGSTRUP, E. (1971): Rocket observation of VLF hiss in aurora. Planet. Space Sci., **19**, 1475–1495.

UNGSTRUP, E. (1975): Narrow band VLF electromagnetic signals generated in the auroral ionosphere by the high-frequency two-stream instability. J. Geophys. Res., **80**, 4272-4278.

UNGSTRUP, E. (1980): Electrostatic waves in the ionosphere. Exploration of the Polar Upper Atmosphere, ed, by C. S. DEEHR and J. A. HOLTET. Dordrecht, D. Reidel, 395–406.

UNGSTRUP, E., NEUBERT, T. and BAHNSEN, A. (1978): Observations on GEOS-1 of 10.2 to 13.6 kHz ground based transmitter signals. Space Sci. Rev., **22**, 453–464.

(Received June 30, 1986; Revised manuscript received January 21, 1987)